

Comparative phosphoproteome analysis to identify candidate phosphoproteins involved in blue light-induced brown film formation in *Lentinula edodes*

Tingting Song¹, Yingyue Shen¹, Qunli Jin¹, Weilin Feng¹, Lijun Fan¹, Weiming Cai^{Corresp. 1}

¹ Institute of Horticulture, Zhejiang Academy of Agricultural Sciences, Hangzhou, China

Corresponding Author: Weiming Cai
Email address: caiwm0527@126.com

Light plays an important role in the growth and differentiation of *Lentinula edodes* mycelia, and mycelial morphology is influenced by light wavelengths. The blue light-induced formation of brown film on the vegetative mycelial tissues of *L. edodes* is an important process. However, the mechanisms of *L. edodes*' brown film formation, as induced by blue light, are still unclear. Using a high-resolution liquid chromatography-tandem mass spectrometry integrated with a highly sensitive immune-affinity antibody method, phosphoproteomes of *L. edodes* mycelia under red- and blue-light conditions were analyzed. A total of 11,224 phosphorylation sites were identified on 2,786 proteins, of which 9,243 sites on 2,579 proteins contained quantitative information. In total, 475 sites were up-regulated and 349 sites were down-regulated in the blue vs red group. To characterize the differentially phosphorylated proteins, systematic bioinformatics analyses, including gene ontology annotations, domain annotations, subcellular localizations, and Kyoto Encyclopedia of Genes and Genomes pathway annotations, were performed. These differentially phosphorylated proteins were correlated with light signal transduction, cell wall degradation, and melanogenesis, suggesting that these processes are involved in the formation of the brown film. Our study provides new insights into the molecular mechanisms of the blue light-induced brown film formation at the post-translational modification level.

1

2 **Comparative phosphoproteome analysis to identify**
3 **candidate phosphoproteins involved in blue light-**
4 **induced brown film formation in *Lentinula edodes***

5

6

7 Tingting Song¹, Yingyue Shen¹, Qunli Jin¹, Weilin Feng¹, Lijun Fan¹, Weiming Cai^{1*}

8

9 ¹Institute of Horticulture, Zhejiang Academy of Agricultural Sciences, Hangzhou, Zhejiang,
10 China

11

12 Corresponding author:

13 Weiming Cai

14 198 Shiqiao road, Hangzhou, Zhejiang, 310021,China

15 E-mail: CaiWM527@126.com;

16

17

18

19

20

21

22

23

24

25

26

27

28

29

30

31

32

33

34 Abstract:

35 Light plays an important role in the growth and differentiation of *Lentinula edodes* mycelia, and
36 mycelial morphology is influenced by light wavelengths. The blue light-induced formation of
37 brown film on the vegetative mycelial tissues of *L. edodes* is an important process. However, the
38 mechanisms of *L. edodes*' brown film formation, as induced by blue light, are still unclear. Using
39 a high-resolution liquid chromatography-tandem mass spectrometry integrated with a highly
40 sensitive immune-affinity antibody method, phosphoproteomes of *L. edodes* mycelia under red-
41 and blue-light conditions were analyzed. A total of 11,224 phosphorylation sites were identified
42 on 2,786 proteins, of which 9,243 sites on 2,579 proteins contained quantitative information. In
43 total, 475 sites were up-regulated and 349 sites were down-regulated in the blue vs red group. To
44 characterize the differentially phosphorylated proteins, systematic bioinformatics analyses,
45 including gene ontology annotations, domain annotations, subcellular localizations, and Kyoto
46 Encyclopedia of Genes and Genomes pathway annotations, were performed. These differentially
47 phosphorylated proteins were correlated with light signal transduction, cell wall degradation, and
48 melanogenesis, suggesting that these processes are involved in the formation of the brown film.
49 Our study provides new insights into the molecular mechanisms of the blue light-induced brown
50 film formation at the post-translational modification level.

51

52 Keywords: brown film formation; *Lentinula edodes*; light sensing; mycelia; phosphorylation;
53 post-translational modification

54

55

56

57

58

59

60

61

62

63

64

65

66

67

68

69

70

71 INTRODUCTION

72 *Lentinula edodes*, also known as shiitake mushroom, belonging to *Lentinus*, is a valuable
73 medicinal and edible fungus(Ozcelik & Peksen 2007). It is a popular edible mushroom and the
74 third most cultivated mushroom in the world(Philippoussis et al. 2000). During cultivation, there

75 are at least four growth stages: vegetative mycelial growth with growth substrate colonization,
76 the light-induced brown film formation, primordial formation, and fruiting body
77 development(Aleksandrova et al. 1998). The brown film formation on the surface of mature
78 mycelia usually appears on the fruiting body primordia and may represent a speciation
79 step(Aleksandrova et al. 1998; Chum et al. 2008; Tsvileva et al. 2005). In addition, the mycelial
80 surface does not form a brown film, which is easily occupied by pathogenic organisms, such as
81 bacteria, green molds and fungi(Koo et al.). Light signals are essential factors in the formation of
82 brown films(Tang et al. 2013; Yin et al. 2017; Zhang et al. 2015). The basic genetic regulatory
83 mechanisms of brown film formation and the influence of environmental factors, especially light,
84 remain unclear. Comparative transcriptome studies revealed that the mechanisms of light-
85 induced brown film formation are related to photosensitivity, signal transduction pathways, and
86 melanin deposition(Tang et al. 2013). Several gene ontology (GO) classifications related to
87 brown film formation were revealed by two-dimensional electrophoresis combined with the
88 matrix-assisted laser desorption/ionization tandem time-of-flight mass spectrometry approach
89 and included small molecule metabolic processes, response to oxidative stress, and organic
90 substance catabolic processes(Tang et al. 2016). Jim et al. compared the morphological changes
91 and gene expression of *Lentinus edodes* under blue light and continuous dark conditions. Their
92 results indicated that the differential genes were involved in the morphological development of
93 primordia and embryonic muscle, cell adhesion and the structure of cellulose and non-cellulose
94 cell walls that affect the development of fruiting bodies, as well as photoreceptors of blue light
95 signals for fruiting body development and pigment formation (Kim et al,2020). Blue light is an
96 important environmental factor in inducing primordial differentiation and the fruiting body
97 development of mushrooms, such as *Hypsizygus marmoreus*, *Pleurotus ostreatus*, and *Coprinus*
98 *cinereus*(Kues et al. 1998; Terashima et al. 2005; Xie et al. 2018).

99 During the growth and development of fungi, the influence of light is very important, and it is
100 also necessary for their growth and development(Crosson et al. 2003). As an external signal,
101 light regulates mycelial growth, primordial differentiation, fruiting body formation, gene
102 expression, and metabolite and enzyme activities through complex light-sensing systems(Cohen
103 et al. 2013; Miyake et al. 2005; Wu et al. 2013; Zhang et al. 2013). At least 100 kinds of fungi
104 have light-perception systems, including red, blue, green, and near-violet(Casas-Flores et al.
105 2006). Photoreceptors are proteins that harvest light and produce signals that are then transported
106 to the nucleus to activate the transcription of light-responsive genes(Hurley et al. 2012). The
107 white collar-1/white collar-2 (WC-1/WC-2) complex is the main blue-light sensor in *Neurospora*

108 *crassa*, a model organism for studying photoperiod(Dunlap 2006; Linden & H.). Other blue-light
109 receptors have been successfully identified and cloned, such as the *dst1* and *dst2* genes in *C.*
110 *cinereus*, *phrA* and *phrB* in *L. edodes*, *Cmwc-1* in different strains of *Cordyceps militaris*, and
111 *Slwc-1* from *Sparassis latifolia*(Kuratani et al. 2010; Sano et al. 2009; Sano et al. 2007;
112 Terashima et al. 2005; Yang et al. ; Yang et al. 2012). However, the molecular mechanisms of
113 blue light-induced brown film formation are still unknown.

114 With the determinations and in-depth analyses of genome and transcriptome sequences of
115 model organisms, such as *Arabidopsis thaliana*, researchers have realized that it is impossible to
116 understand the functions of organisms from only a gene-based perspective(Abbott 2001).
117 Proteomics studies the compositions, expressions, structures, functions, interactions between
118 proteins and their activities(Graves & Haystead 2002). Isobaric tags for relative and absolute
119 quantification/tandem mass tag (iTRAQ/TMT)-labeling combined with tandem mass
120 spectrometry is a high-throughput quantitative proteomics application technology developed in
121 recent years(Zhan et al. 2019). Compared with relatively stable genomes, proteins are diverse
122 and changeable. In addition, the presence of post-translational modifications (PTMs) and protein
123 processing, such as phosphorylation, glycosylation, and acetylation, are not comparable at the
124 genome or RNA level(Piehler 2005). Proteomics research is a cutting-edge technique in the
125 edible fungi industry. With the effects of abiotic stresses on protein expression levels have been
126 studied the most(Hernandez-Macedo et al. 2002; Liang et al. 2007).

127 In this study, an immunoaffinity analysis combined with high-resolution liquid
128 chromatography-tandem mass spectrometry (LC-MS/MS) was used to study the global
129 phosphorylated proteome of brown films induced by blue light. This study provides new insights
130 into the molecular mechanisms of blue light-induced brown film formation at the PTM level.

131

132 **Materials and Methods**

133 **Materials treatment and protein extraction**

134 The *L. edodes* strain L901 which is a new hybrid strain was obtained from the Zhejiang
135 Academy of Agricultural Sciences. Fungal mycelia were grown at 22°C under red- and blue-light
136 conditions (LED light sources) for 22 d. The light intensity approximately 100 lux and the
137 incubator illuminated all day. Fungal mycelia were grown were grown in the potato dextrose

138 agar media. Samplings were taken after mycelial changed colour under blue light conditions. The
139 determination of total polysaccharides was performed according to Zhang's description (*Zhang et*
140 *al. 2018*). For protein extraction, a proper amount of sample was ground in liquid nitrogen into a
141 cellular powder and then transferred to a 5-mL centrifuge tube. The samples were treated with
142 four volumes of lysis buffer (10 mM dithiothreitol, 1% protease inhibitor, and 1% phosphatase
143 inhibitor) and then sonicated three times. The supernatant was centrifuged for 10 min at 4°C and
144 5,500 g with an equal volume of Tris equilibrium phenol. The supernatant was taken and
145 precipitated overnight with a fivefold volume of 0.1 M ammonium acetate/methanol. The protein
146 precipitation was washed sequentially with methanol and acetone. The protein was redissolved in
147 8 M urea, and the protein concentration was determined using a bicinchoninic acid assay kit
148 (P0012, Beyotime, Shanghai, China) according to the manufacturer's instructions.

149 **Trypsin digestion, TMT labeling, and HPLC fractionation**

150 For digestion, the final concentration of dithiothreitol in the protein solution was 5 mM and was
151 reduced at 56°C for 30 min. The 11-m final concentration of iodoacetamide was incubated at
152 room temperature for 15 min. Finally, the urea concentration of the sample was diluted to less
153 than 2 M. Trypsin was added at 1:50 trypsin-to-protein mass ratio for the first digestion
154 overnight and 1:100 trypsin-to-protein mass ratio for a second 4 h-digestion. The trypsinase-
155 hydrolyzed peptide segments were desalted using a Strata X C18 (Phenomenex) and then freeze-
156 dried in a vacuum. The peptide segment was dissolved in 0.5 M Triethylammonium bicarbonate
157 and labeled according to the instructions of the TMT kit(90066, Thermo-Scientific, Rockford, IL,
158 USA). The simple operation was as follows: the labeled reagent was dissolved in acetonitrile
159 after thawing, incubated at room temperature for 2 h after mixing with the peptide segment,
160 desalinated after mixing with the labeled peptide segment, and freeze-dried in a vacuum.

161 The tryptic peptides were fractionated using high pH reverse-phase HPLC on an Agilent
162 300Extend C18 column (5- μ m particles, 4.6-mm ID, 250-mm length). Briefly, peptides were first
163 separated using a gradient of 8% to 32% acetonitrile (pH 9.0) over 60 min into 60 fractions.
164 Then, the peptides were combined into six fractions and dried by vacuum centrifugation.

165

166 **Affinity enrichment**

167 Peptide mixtures were first incubated with an immobilized metal ion affinity chromatography
168 (IMAC) microsphere suspension and vibrated in loading buffer (50% acetonitrile and 6%
169 trifluoroacetic acid). IMAC microspheres were used Ti. The IMAC microspheres enriched with
170 phosphopeptides were collected by centrifugation, and the supernatant was removed. To remove
171 nonspecifically adsorbed peptides, the IMAC microspheres were washed with loading buffer and
172 30% acetonitrile plus 0.1% trifluoroacetic acid, sequentially. To elute the enriched
173 phosphopeptides from the IMAC microspheres, elution buffer containing 10% NH₄OH was
174 added, and the enriched phosphopeptides were eluted with vibration. The resulting peptides were
175 desalted with C18 ZipTips (Millipore) and lyophilized for the LC-MS/MS analysis.

176

177 **LC-MS/MS analysis**

178 The tryptic peptides were dissolved in 0.1% formic acid and directly loaded onto a home-made
179 reversed-phase analytical column (15-cm length and 75- μ m i.d.). The gradient increased from
180 6% to 23% solvent B (0.1% formic acid in 98% acetonitrile) over 26 min, 23% to 35% in 8 min
181 and to 80% in 3 min. It was then held at 80% for the last 3 min, at a constant flow rate of 400
182 nL/min on an EASY-nLC 1000 UPLC system.

183 The peptides were subjected to an NSI source followed by MS/MS in Q ExactiveTM Plus
184 (Thermo) coupled online to the UPLC. The electrospray voltage applied was 2.0 kV. The m/z
185 scan range was 350 to 1,800 for a full scan, and intact peptides were detected in the Orbitrap at a
186 resolution of 70,000. Peptides were then selected for MS/MS using normalized collision energy
187 (NCE) set as 28, and the fragments were detected in the Orbitrap at a resolution of 17,500. The
188 data-dependent procedure alternated between one MS scan and 20 MS/MS scans with a 15.0-s
189 dynamic exclusion. The automatic gain control was set at 5E4. The fixed first mass was set as
190 100 m/z.

191

192 **Database search**

193 The MS data were retrieved using Maxquant (v1.5.2.8) using the following search parameter
194 settings: the database was Lentinula_edodes_uniprot
195 (<https://www.uniprot.org/proteomes/?query=organism:5353&sort=score>); an anti-database was

196 added to calculate the false positive rate (FDR) caused by random matching and a common
197 contamination library was added to eliminate the contamination proteins from the results.
198 Trypsin/P was specified as the cleavage enzyme, allowing up to four missing cleavage events.
199 The mass tolerance for precursor ions was set as 20 ppm in the first search and 5 ppm in the main
200 search, and the mass tolerance for fragment ions was set as 0.02 Da. Carbamidomethyl on Cys
201 was specified as a fixed modification, and acetylation and oxidation of Met were specified as
202 variable modifications. The FDR was adjusted to < 1%, and the minimum score for modified
203 peptides was set > 40.

204

205 **Annotation methods and functional enrichment**

206 The GO annotation on the proteomics level was derived from the UniProt-GOA database
207 (<http://www.ebi.ac.uk/GOA/>). First, the system converted the protein ID to UniProt ID, matched
208 the GO ID with the UniProt ID, and then extracted the corresponding information from the
209 UniProt-GOA database based on the GO ID. If there was no protein information queried in the
210 UniProt-GOA database, then algorithm software based on the protein sequence, InterProScan,
211 was used to predict the GO function of the protein.

212 The KEGG database was used to annotate protein pathways. First, the KEGG online service
213 tool KAAS was used to annotate the submitted proteins, and then KEGG mapper was used to
214 place the annotated proteins into the corresponding pathways in the database. WoLF PSORT, a
215 software for predicting subcellular localization, was used to annotate the submitted proteins for
216 subcellular localization. Fisher's exact test was used to detect differentially modified proteins
217 against the background of identified proteins. A P-value of less than 0.05 was considered
218 significant. The softwares motif-x and MoMo were used to analyze the models of sequences that
219 contained the amino acids in specific positions of modified 13-mers (six amino acids upstream
220 and downstream of the site) in all the protein sequences.

221

222 **Results**

223 **Characteristics of quantitative phosphoproteomic data in *L. edodes* mycelia**

224 Using affinity enrichment followed by LC-MS/MS, the phosphoproteomic changes in *L. edodes*
225 mycelia grown in red or blue light were investigated. A flow chart of our experiment is exhibited

226 in Fig. 1A. Pearson's correlation coefficient between the two groups showed sufficient
227 reproducibility (Fig. 1B). In this study, 160,949 secondary spectra were obtained by MS
228 analyses. After searching the theoretical protein data, the effective number of spectra was 22,857
229 and the utilization rate of the spectra was 14.2%. In total, 8,830 peptides and 7,777
230 phosphorylated peptides were identified. There were 11,224 phosphorylation modification sites
231 on 2,786 proteins, of which 9,243 sites on 2,579 proteins provided quantitative information
232 (Fig. 1C). The first-order mass errors of most spectra are less than 10 ppm, which is in
233 accordance with the high accuracy of the MS (Fig. 1D). Most of the peptides were distributed in
234 7–20 amino acids, which was in accordance with the general rules of trypsin-based enzymatic
235 hydrolysis and high energy collision dissociation (HCD) fragmentation, indicating that the
236 sample preparation and the quality accuracy of the mass spectrometer reached the standard
237 required (Fig. 1E). The detailed information regarding the identified peptides are listed in Table
238 S1.

239

240 **Analysis of phosphorylation sites**

241 In *L. edodes* mycelia, 977 (35.07%) phosphoproteins were modified at a single site, 519
242 (18.63%) at two sites, and 1,290 (46.3%) at three or more phosphosites (Fig. 2A). Interestingly,
243 some proteins contained a large number of phosphosites. For example, there are 34 phosphosites
244 in a non-specific serine/threonine protein kinase (A0A1Q3E061), 45 phosphosites in a regulatory
245 transcript from a polymerase II promoter-related protein (A0A1Q3ERS8) and 53 phosphosites in
246 a SRC Homology 3 (Sh3) domain-containing protein (A0A1Q3ENM7) (Table S1).

247 To analyze the density levels of the phosphorylation sites in each protein, the phosphorylated
248 proteome of *L. edodes* was compared with those of other species. The average number of
249 phosphorylation sites per protein in *L. edodes* is 3.22, which is similar to the numbers in *Bombyx*
250 *mori* (3.07), *Nicotiana tabacum* (3.05), and *Physcomitrella patens* (3.44) (Fig. 2B) (Fang et al.
251 2016; Lu et al. 2019; Shobahah et al. 2017).

252 **Characteristics of the identified phosphoproteins in *L. edodes***

253 To predict the possible functions of the identified phosphoproteins, a GO classification analysis
254 was performed. Most of the proteins were classified into three GO categories (Fig. 3A).
255 Specifically, 594 proteins were annotated as 'metabolic process', 519 proteins were annotated as
256 'cellular process', and 361 proteins were annotated as 'single-organism process'. In the cellular

257 component category, the largest terms were ‘cell’ (289 proteins), ‘organelle’ (186 proteins), and
258 ‘macromolecular complex’ (154 proteins). In the molecular function category, ‘binding’ (846
259 proteins), ‘catalytic activity’ (627 proteins), and ‘transporter activity’ (51 proteins) were the three
260 top dominant terms. The euKaryotic Ortholog Groups annotation clustered all the
261 phosphoproteins into four major categories. The ‘cellular processes and signaling’ category
262 contained the largest number of proteins(Fig.3B). Most identified phosphoproteins were grouped
263 into 13 subcellular component categories predicted by WoLF PSORT software, including 783
264 nuclear, 380 cytoplasmic, and 275 mitochondrial proteins(Fig.3C). The detailed annotation
265 information for all the identified phosphoproteins are listed in Table S2.

266

267 **Protein motifs associated with phosphorylation**

268 Among the identified phosphosites in *L. edodes*, 8,645 sites occurred at serine residues, 2239
269 sites at threonine residues, and 340 sites at tyrosine residues (Fig.4A). To understand the
270 upstream pathway of the identified phosphorylated proteins, a motif analysis was carried out
271 using MOMO and Motif-X software. A number of conserved phosphorylation motifs were
272 enriched in the phosphorylated proteins of *L. edodes* (Table S3). A total of 7,741 distinct
273 sequences containing 13 residues were obtained, with 6 upstream and 6 downstream residues
274 around each phosphosite (Table S4). The five S-based motifs containing the largest numbers of
275 sequences were ‘sP’, ‘RxxsP’, ‘PxsP’ ‘Gs’, and ‘RRxS’, and the five top T-based motifs were
276 ‘tP’, ‘tPP’, ‘RxxtP’, ‘RxtP’, and ‘Rxxt’. A Y-based motif, ‘Rxxxxxy’, was identified. Two
277 position-specific heat maps of upstream and downstream amino acids at all the identified
278 phosphorylated serine or threonine sites. For the S-based motifs, strong preferences for glutamic
279 acid, lysine, and arginine upstream, and aspartic acid, glutamic acid, and proline downstream, of
280 the phosphorylation sites were observed. For the T-based motifs, preferences for lysine, proline,
281 and arginine upstream, and aspartic acid and proline downstream, of the phosphorylation sites
282 were observed (Fig. 4C).

283

284 **Differentially phosphorylated proteins (DPPs) in response to a blue-light treatment**

285 To compare the DPPs between red- and blue-light treated samples, expression profiles of the
286 proteins generated by MeV software are shown in a heatmap (Fig. 5A). The screening of DPPs
287 followed the following criteria: change threshold ≥ 1.5 times and t-test p-value < 0.05 . Among

288 these DPPs, 475 sites in 317 phosphorylated proteins were up-regulated and 349 sites in 243
289 phosphorylated proteins were down-regulated (Fig. 5B and Table S5). Based on the subcellular
290 localizations predicted by WoLF PSORT software, all the DPPs were classified into 10
291 subcellular components. There were 204 nuclear localized DPPs, 82 cytoplasmic localized DPPs,
292 and 51 plasma membrane localized DPPs (Fig. 5C).

293

294 **Functional enrichment analysis of the DPPs**

295 To understand the biological functions of these phosphorylated proteins, GO, KEGG and protein
296 domain enrichment analyses of DPPs were carried out. For biological process, cellular
297 component, and molecular function categories, the DPPs were mostly enriched in ‘DNA
298 conformation change’ (Fig. 6A); ‘nucleosome’ (Fig. 6B), and ‘transporter activity’ (Fig. 6C),
299 respectively.

300 To reveal the metabolic pathways involved in the formation of brown films induced by blue
301 light, the DPPs were further analyzed using the KEGG database. For the up-regulated DPPs, two
302 KEGG pathways, ‘Ribosome biogenesis in eukaryotes’, and ‘ABC transporters’, were
303 significantly enriched’ (Fig. 7A). For the down-regulated DPPs, four enriched KEGG pathways
304 were identified, ‘Valine, leucine and isoleucine degradation’, ‘Phenylalanine metabolism’,
305 ‘Galactose metabolism’, and ‘Fructose and mannose metabolism’ (Fig. 7B). We also found that
306 the total polysaccharides of blue light treatment was significantly lower than that of red light
307 treatment (Fig. S1). A protein domain enrichment analysis revealed that the up-regulated DPPs
308 were enriched in 19 protein domains, with ‘ABC transporter-like’, ‘P-type ATPase’, and ‘HAD-
309 like domain’ being the most highly enriched (Fig. 7C). The down-regulated DPPs were most
310 strongly associated with ‘Glutathione S-transferase, C-terminal-like’, ‘YTH domain’ ‘VPS9
311 domain’, ‘Domain of unknown function DUF1708’, and ‘High mobility group box domain’ (Fig.
312 7D).

313

314 **Identification of DPPs related to signal transduction mechanisms and carbohydrate-active 315 enzymes (CAZymes)**

316 To better understand the DPPs related to blue light-induced mycelial brown film formation, a
317 functional classification of DPPs was conducted using euKaryotic Ortholog Groups. A total of

318 319 DDPs were grouped into 23 subcategories (Fig. S2). For the ‘signal transduction
319 mechanisms’ subcategory, 50 phosphosites in 29 phosphorylated proteins were identified (Table
320 1). Among these, 30 phosphosites were up-regulated and 20 were down-regulated.

321 CAZymes, including auxiliary activity (AA), carbohydrate-binding modules (CBM),
322 carbohydrate esterase (CE), glycoside hydrolase (GH), glycosyl transferase (GT), and
323 polysaccharide lyase (PL), were involved in the hydrolysis of plant cell wall polysaccharides and
324 play an important role in the degradation of substrates (Davies & Williams 2016). In the present
325 study, 13 DPPs were identified as CAZymes, including 11 phosphosites in three CBMs, two
326 phosphosites in two CEs, four phosphosites in three GHs, and six phosphosites in five GTs (Table
327 2). Interestingly, the GHs were up-regulated, while the CBMs were down-regulated.

328

329 Discussion

330 With the completion of various biological genome sequences, proteomics has become an
331 increasingly important analysis of important proteins based on the differential recognition of
332 their expression levels. Protein phosphorylation is an important PTM, which can rapidly control
333 enzyme activity, subcellular localization, and protein stability, and involves the regulation of
334 metabolism, transcription, and translation, as well as protein degradation, homeostasis, cell
335 signaling, and communication (Lv *et al.* 2014; Thingholm *et al.* 2009; Yu *et al.* 2019). Recently,
336 large-scale quantitative phosphoproteomics analyses were performed in many plants to elucidate
337 the growth, development, and diverse response mechanisms, but the technology has rarely been
338 applied to *L. edodes* (Lv *et al.* 2014). Here, we report a comprehensive analysis of
339 phosphoproteomic responses to blue light-induced mycelial brown film formation of *L. edodes*
340 through a combination of affinity enrichment and LC-MS/MS.

341 Protein phosphorylation is a common PTM, but the level of phosphorylation varies with
342 species. The number of phosphorylation sites in each protein is 3.22, which is higher than most
343 published phosphorylation proteomes, indicating that the degree of phosphorylation in the *L.*
344 *edodes* proteome is very high. The large number of identified phosphoproteins provide an
345 opportunity to comprehensively analyze the mechanism of blue light-induced mycelial brown
346 film formation. The ‘sP’ motif most frequently occurred in many species, including *L.*
347 *edodes* (van Wijk *et al.* 2014; Wang *et al.* 2014; Zhang *et al.* 2014). ‘sP’ is a target of the
348 following kinases: cyclin-dependent kinase, mitogen-activated protein kinase (MAPK), and

349 sucrose non-fermenting1-related protein kinase 2(*van Wijk et al. 2014; Zhang et al. 2014*). The
350 ‘tP’ motif also provides a target for MAPKs(*Wang et al. 2013*).

351 In Basidiomycetes, light is a crucial environmental factor that affects fruiting body induction
352 and development(*Kues 2000; Kues & Liu 2000*). In recent years, in fungi, the effects of different
353 light wavelengths on mycelial morphology, metabolites, and enzymatic activities have been
354 studied. In *Monascus*, red and blue light can affect the formation of mycelia and spores, as well
355 as the production of secondary metabolites(*Miyake et al. 2005*). In this study, we found that blue
356 light can promote the formation of a brown film associated with *L. edodes* mycelia, but no
357 correlation was found with a red-light treatment. The effects of blue light on the expression
358 levels of phosphorylated proteins during brown film formation were studied. Phosphorylation
359 proteomics revealed that 560 phosphorylated proteins were differentially expressed during a
360 blue-light treatment.

361 Brown film formation at the transcriptional level is correlated with photoreceptor activity,
362 light signaling pathways, and pigment formation(*Tang et al. 2013*). Most fungi perceive blue
363 light through homologues of the white collar complex, which is a complex of photoreceptors and
364 transcription factors that was first found in *Neurospora crassa*(*Tagua et al. 2015*). The N-
365 terminus of WC-1 is a lov domain, which is a special Per-Arnt-Sim (PAS) domain that can bind
366 to flavin adenine dinucleotide(*Crosson et al. 2003*). Light sensing via photoreceptors such as
367 FMN- and FAD-bindings and signal transduction by kinases and G protein-coupled receptors
368 were identified as differential expression genes specific to the light-induced brown film
369 phenotypes(*Yoo et al, 2019*). In the present study, three flavin adenine dinucleotide-binding
370 domains and an FMN-binding domain differentially accumulated, indicating that the *L. edodes*
371 mycelia could have perceived blue light when the brown film was formed. The MAPK cascade is
372 an important signal transduction pathway connecting light responses and the biological clock(*de*
373 *Paula et al. 2008*). MAPK also regulates various secondary metabolic activities in *Aspergillus*
374 *nidulans* and *Colletotrichum lagenarium*, and it controls light-influenced melanin biosynthesis in
375 *B. cinerea*(*Atoui et al. 2008; Bayram & Braus 2012; Liu et al. 2011; Takano et al. 2000*). The
376 MAPK signal transduction pathways may be directly involved in brown film formation(*Tang et*
377 *al. 2013*). Several MAPK signal transduction pathways related to DPPs were identified in this
378 study, suggesting that these signal pathways are involved in the formation of brown films.

379 The differential expression of CAZymes were observed in *L. edodes* mycelia under two light
380 conditions. GHs mainly hydrolyze glycosidic bonds between carbohydrates or between

381 carbohydrates and non-carbohydrates(*Sathya & Khan 2014*). The GH61 family contains copper-
382 dependent lytic polysaccharide monooxygenase(*Langston et al. 2011*). CEs catalyze the
383 deacylation of esters or amides, in which sugar plays the role of alcohol and amine(*Biely 2012*;
384 *Vidal-Melgosa et al. 2015*). They are currently divided into 16 different families, which have a
385 great diversity in substrate specificity and structure(*Vidal-Melgosa et al. 2015*). CE10 (two
386 DPPs) were down-regulated by blue light. CBMs are noncatalytic, individually folded domains
387 that are attached to the catalytic enzyme modules by linkers(*Varnai et al. 2014*). Some CE1
388 enzymes may contain a CBM48 family protein, which is associated with starch binding(*Wilkens*
389 *et al. 2017*; *Wong et al. 2017*). Our research showed that these CAZymes play important roles in
390 the degradation of lignocellulose and provide sufficient nutrition for the formation of the brown
391 film of mushroom mycelia.

392 To survive, fungi have evolved the ability to adapt to different environmental conditions, and
393 various metabolic pathways secrete different metabolites(*Yu & Keller 2005*). The regulation of
394 these metabolites is not only related to fungal growth and development, but also to light
395 stimulation and responses. The shorter the light wavelength, the more polysaccharides
396 accumulated in the cells of *Pleurotus eryngii*(*Jang et al. 2011*). Blue-light treatments
397 significantly improved the synthesis of ergosterol and polyphenols in the fruiting body of
398 *Pleurotus eryngii*, and the scavenging ability of the free radicals was the greatest compared with
399 other light treatments(*Jang et al. 2011*). In our study, the KEGG-enrichment analysis showed
400 that four DPPs belonged to ‘Galactose metabolism’ and ‘Fructose and mannose metabolism’,
401 suggesting that the blue light affected the sugar metabolism of *L. edodes*. Phenolic compounds
402 were correlated with pigment formation(*Weijn et al. 2013*). Phenylalanine ammonia-lyase and
403 tyrosinase-encoding genes were significantly up-regulated in *P. eryngii* under blue-light
404 conditions(*Du et al. 2019*). Two ‘Phenylalanine metabolism’ pathway phosphoproteins, amidase
405 (A0A1Q3E9W2) and aspartate aminotransferase (A0A1Q3EG41), were down-regulated in
406 mycelia under blue-light conditions. These results suggested that blue light may promote the
407 formation of melanin and inhibit the formation of other phenolic compounds. Polyketide
408 synthase (PKS) is an essential enzyme in the biosynthesis of fungal secondary metabolites(*Austin*
409 *& Noel 2003*; *Linnemannstons et al. 2002*). PKSs modify the polyketide backbone with other
410 enzymes, such as Cytochrome P450 monooxygenases, oxidoreductase, and
411 omethyltransferase(*Austin & Noel 2003*). P450-linked monooxygenases mediate oxidation–
412 reduction steps in aflatoxin biosynthesis, and omethyltransferase was involved in yellow pigment
413 biosynthesis through an aflatoxigenic *Aspergillus* strain(*Bhatnagar et al. 2003*). In our study, the

414 phosphorylation levels of PKS, O-methyltransferase, P450 monooxygenase, and oxidoreductase
415 changed in brown film formation, indicating that they may play roles in pigment production.

416 The ABC transport family is widely distributed in all living species, including several
417 subfamilies, which are responsible for different types of material transport
418 (Higgins.2001;Holland and Blight. 1999). ATPase is the largest ATP dependent ion transporter
419 in organisms, transporting many different ions, metals and other substrates (*Palmgren & Nissen,*
420 *2011*). Two VPS9 domain containing proteins, Rab5 GDP/GTP exchange factor, were down-
421 regulated under blue light treatment. Studies have shown that the transport of endocytic vesicles
422 is partially regulated by Rab protein (*Zhu et al, 2018*).Rab protein needs to be activated by
423 guanine nucleotide exchange factor, which transforms Rab from a GDP binding state to a GTP
424 binding state(*Zerial,2001*).The changed in these proteins suggest that blue light altered the
425 transport of certain substances. In mushrooms, blue light can promote growth, which is
426 considered to be an important environmental factor affecting the growth of fruiting bodies(*Yoo et*
427 *al, 2019*).In this study, ribosome biogenesis related proteins were observed to be up-regulated
428 under blue light treatment.

429

430 **Conclusions**

431 Using a high-resolution LC-MS/MS integrated with a highly sensitive immune-affinity antibody
432 method, phosphoproteomes of *L. edodes* mycelia under red- and blue-light conditions were
433 analyzed. In this study, 11,224 phosphorylation sites were identified on 2,786 proteins, of which
434 9,243 sites on 2,579 proteins contained quantitative information. In total, 475 sites were up-
435 regulated and 349 sites were down-regulated in the blue vs red group. Then, we carried out a
436 systematic bioinformatics analyses of proteins containing quantitative information sites,
437 including protein annotations, functional classifications, and functional enrichments. Our study
438 provides new insights into the molecular mechanisms of the blue light-induced brown film
439 formation at the PTM level

440

441 **Acknowledgments**

442 We are grateful to the PTM Biolabs company for technical support. We thank International
443 Science Editing for editing this manuscript(<http://www.internationalscienceediting.com>)

444

445 **ADDITIONAL INFORMATION AND DECLARATIONS**

446

447 **Funding**

448 This study was supported by the Zhejiang Science and Technology Major program on
449 Agriculture New Variety Breeding (Grant No.2016C02057) and National Science Foundation of
450 Zhejiang Province of China (Grant No.LQ16C150004). The funders had no role in study design,
451 data collection and analysis, decision to publish, or preparation of the manuscript.

452

453 **Grant Disclosures**

454 The following grant information was disclosed by the authors:

455 Zhejiang Science and Technology Major program on Agriculture New Variety Breeding:
456 2016C02057.

457 National Science Foundation of Zhejiang Province of China: Grant No.LQ16C150004.

458

459 **Competing interests**

460 The authors declare that they have no competing interests.

461

462 **Author Contributions**

463 • Tingting Song and Weiming Cai conceived and designed the experiments, performed the
464 experiments, analyzed the data, prepared figures and/or tables, authored or reviewed drafts of the
465 paper, approved the final draft.

466 • Yingyue Shen and Qunli Jin Weilin Feng performed the experiments, analyzed the

467 data, approved the final draft.

468 • Weilin Feng and Lijun Fan performed the experiments, analyzed the data, prepared figures
469 and/or tables, approved the final draft, comparative experimental data.

470

471 **Data Availability**

472 The following information was supplied regarding data availability:

473 The raw data is available at ProteomeXchange:PX016536

474

475 **References**

476 Abbott A. 2001. And now for the proteome. *Nature* 409:747-747.

477 Aleksandrova EA, Zav'yalova LA, Tereshina VM, Garibova LV, and Feofilova EP. 1998.
478 Obtaining of fruiting bodies and submerged mycelium of *Lentinus edodes* (Berk.) Sing
479 [*Lentinula edodes* (Berk.) Pegler]. *Microbiology* 67:535-539.

480 Atoui A, Bao DP, Kaur N, Grayburn WS, and Calvo AM. 2008. *Aspergillus nidulans* natural
481 product biosynthesis is regulated by mpkB, a putative pheromone response mitogen-
482 activated protein kinase. *Applied And Environmental Microbiology* 74:3596-3600.

483 Austin MB, and Noel AJP. 2003. The chalcone synthase superfamily of type III polyketide
484 synthases. *Natural Product Reports* 20:79-110.

485 Bayram O, and Braus GH. 2012. Coordination of secondary metabolism and development in
486 fungi: the velvet family of regulatory proteins. *Fems Microbiology Reviews* 36:1-24.

487 Bhatnagar D, Ehrlich KC, and Cleveland TE. 2003. Molecular genetic analysis and regulation of
488 aflatoxin biosynthesis. *Applied Microbiology and Biotechnology* 61:83-93.

489 Biely P. 2012. Microbial carbohydrate esterases deacetylating plant polysaccharides.
490 *Biotechnology Advances* 30:1575-1588.

491 Casas-Flores S, Rios-Momberg M, Rosales-Saavedra T, Martinez-Hernandez P, Olmedo-Monfil
492 V, and Herrera-Estrella A. 2006. Cross talk between a fungal blue-light perception
493 system and the cyclic AMP signaling pathway. *Eukaryotic Cell* 5:499-506.

- 494 Chum WW, Ng KT, Shih RS, Au CH, and Kwan HS. 2008. Gene expression studies of the
495 dikaryotic mycelium and primordium of *Lentinula edodes* by serial analysis of gene
496 expression. *Mycol Res* 112:950-964.
- 497 Cohen Y, Vaknin M, Ben-Naim Y, and Rubin AE. 2013. Light Suppresses Sporulation and
498 Epidemics of *Peronospora belbahrii*. *Plos One* 8.
- 499 Crosson S, Rajagopal S, and Moffat K. 2003. The LOV domain family: Photoresponsive
500 signaling modules coupled to diverse output domains. *Biochemistry* 42:2-10.
- 501 Davies GJ, and Williams SJ. 2016. Carbohydrate-active enzymes: sequences, shapes, contortions
502 and cells. *Biochemical Society Transactions* 44:79-87.
- 503 de Paula RM, Lamb TM, Bennett L, and Bell-Pedersen D. 2008. A connection between MAPK
504 pathways and circadian clocks. *Cell Cycle* 7:2630-2634.
- 505 Du F, Zou Y, Hu Q, Zhang H, and Ye D. 2019. Comparative transcriptomic analysis reveals
506 molecular processes involved in pileus morphogenesis in *Pleurotus eryngii* under
507 different light conditions. *Genomics*.
- 508 Dunlap JC. 2006. Proteins in the *Neurospora* circadian clockworks. *Journal Of Biological*
509 *Chemistry* 281:28489-28493.
- 510 Fang Y, Zhang Q, Wang X, Yang X, Wang XY, Huang Z, Jiao YC, and Wang J. 2016.
511 Quantitative phosphoproteomics reveals genistein as a modulator of cell cycle and DNA
512 damage response pathways in triple-negative breast cancer cells. *International Journal Of*
513 *Oncology* 48:1016-1028.
- 514 Graves PR, and Haystead TAJ. 2002. Molecular biologist's guide to proteomics. *Microbiology*
515 *And Molecular Biology Reviews* 66:39-+.
- 516 Hernandez-Macedo ML, Ferraz A, Rodriguez J, Ottoboni LMM, and De Mello MP. 2002. Iron-
517 regulated proteins in *Phanerochaete chrysosporium* and *Lentinula edodes*: Differential
518 analysis by sodium dodecyl sulfate polyacrylamide gel electrophoresis and two-
519 dimensional polyacrylamide gel electrophoresis profiles. *Electrophoresis* 23:655-661.
- 520 Higgins CF. 2001. ABC transporters: physiology, structure and mechanism – an overview.
521 *Research in Microbiology* 152:0-210.

- 522 Holland IB, and Blight MA. 1999. ABC-ATPases, adaptable energy generators fuelling
523 transmembrane movement of a variety of molecules in organisms from bacteria to
524 humans. *Journal of Molecular Biology* 293:0-399. Hurley JM, Chen CH, Loros JJ, and
525 Dunlap JC. 2012. Light-Inducible System for Tunable Protein Expression in *Neurospora*
526 *crassa*. *G3-Genes Genomes Genetics* 2:1207-1212.
- 527 Jang MJ, Lee YH, Kim JH, and Ju YC. 2011. Effect of LED Light on Primordium Formation,
528 Morphological Properties, Ergosterol Content and Antioxidant Activity of Fruit Body in
529 *Pleurotus eryngii*. *Korean Journal of Mycology* 39.
- 530 Kim JY, Kim DY, Park YJ, and Jang MJ. 2020. Transcriptome analysis of the edible mushroom
531 *Lentinula edodes* in response to blue light. *Plos One* 15:e0230680.
- 532 Koo CD, Lee SJ, and Lee HY. Morphological Characteristics of Decomposition and Browning
533 of Oak Sawdust Medium for Ground Bed Cultivation of *Lentinula edodes*.
- 534 Kues U. 2000. Life history and developmental processes in the basidiomycete *Coprinus cinereus*.
535 *Microbiology And Molecular Biology Reviews* 64:316-+.
- 536 Kues U, Granado JD, Hermann R, Boulianne RP, Kertesz-Chaloupkova K, and Aebi M. 1998.
537 The A mating type and blue light regulate all known differentiation processes in the
538 basidiomycete *Coprinus cinereus*. *Molecular And General Genetics* 260:81-91.
- 539 Kues U, and Liu Y. 2000. Fruiting body production in basidiomycetes. *Applied Microbiology*
540 *and Biotechnology* 54:141-152.
- 541 Kuratani M, Tanaka K, Terashima K, Muraguchi H, Nakazawa T, Nakahori K, and Kamada T.
542 2010. The *dst2* gene essential for photomorphogenesis of *Coprinopsis cinerea* encodes a
543 protein with a putative FAD-binding-4 domain. *Fungal Genetics And Biology* 47:152-158.
- 544 Langston JA, Shaghasi T, Abbate E, Xu F, Vlasenko E, and Sweeney MD. 2011. Oxidoreductive
545 Cellulose Depolymerization by the Enzymes Cellobiose Dehydrogenase and Glycoside
546 Hydrolase 61. *Applied And Environmental Microbiology* 77:7007-7015.
- 547 Liang Y, Chen H, Tang MJ, and Shen SH. 2007. Proteome analysis of an ectomycorrhizal fungus
548 *Boletus edulis* under salt shock. *Mycol Res* 111:939-946.

- 549 Linden, and H. White collar 2, a partner in blue-light signal transduction, controlling expression
550 of light-regulated genes in *Neurospora crassa*. *Embo Journal* 16:98-109.
- 551 Linnemannstons P, Schulte J, del Mar Prado M, Proctor RH, Avalos J, and Tudzynski B. 2002.
552 The polyketide synthase gene *pk4* from *Gibberella fujikuroi* encodes a key enzyme in
553 the biosynthesis of the red pigment bikaverin. *Fungal Genetics And Biology* 37:134-148.
- 554 Liu WW, Soulie MC, Perrino C, and Fillinger S. 2011. The osmosensing signal transduction
555 pathway from *Botrytis cinerea* regulates cell wall integrity and MAP kinase pathways
556 control melanin biosynthesis with influence of light. *Fungal Genetics And Biology*
557 48:377-387.
- 558 Lu ZS, Chen QS, Zheng QX, Shen JJ, Luo ZP, Fan K, Xu SH, Shen Q, and Liu PP. 2019.
559 Proteomic and Phosphoproteomic Analysis in Tobacco Mosaic Virus-Infected Tobacco
560 (*Nicotiana tabacum*). *Biomolecules* 9.
- 561 Lv DW, Li X, Zhang M, Gu AQ, Zhen SM, Wang C, Li XH, and Yan YM. 2014. Large-scale
562 phosphoproteome analysis in seedling leaves of *Brachypodium distachyon* L. *BMC*
563 *Genomics* 15.
- 564 Miyake T, Mori A, Kii T, Okuno T, Usui Y, Sato F, Sammoto H, Watanabe A, and Kariyama M.
565 2005. Light effects on cell development and secondary metabolism in *Monascus*. *Journal*
566 *Of Industrial Microbiology & Biotechnology* 32:103-108.
- 567 Ozcelik E, and Peksen A. 2007. Hazelnut husk as a substrate for the cultivation of shiitake
568 mushroom (*Lentinula edodes*). *Bioresource Technology* 98:2652-2658.
- 569 Palmgren MG, Nissen P, 2011. P-type ATPases. *Annu Rev Biophys*, 40, pp. 243-
570 266Philippoussis A, Zervakis G, and Griensven LJLDV. 2000. Cultivation of edible
571 mushrooms in Greece: presentation of the current status and analysis of future trends.
572 96:620-627.
- 573 Piehler J. 2005. New methodologies for measuring protein interactions in vivo and in vitro.
574 *Current Opinion In Structural Biology* 15:4-14.
- 575 Sano H, Kaneko S, Sakamoto Y, Sato T, and Shishido K. 2009. The basidiomycetous mushroom
576 *Lentinula edodes* white collar-2 homolog PHRB, a partner of putative blue-light

- 577 photoreceptor PHRA, binds to a specific site in the promoter region of the L-edodes
578 tyrosinase gene. *Fungal Genetics And Biology* 46:333-341.
- 579 Sano H, Narikiyo T, Kaneko S, Yamazaki T, and Shishido K. 2007. Sequence analysis and
580 expression of a blue-light photoreceptor gene, Le.phrA from the basidiomycetous
581 mushroom *Lentinula edodes*. *Bioscience Biotechnology And Biochemistry* 71:2206-2213.
- 582 Sathya TA, and Khan M. 2014. Diversity of Glycosyl Hydrolase Enzymes from Metagenome
583 and Their Application in Food Industry. *Journal Of Food Science* 79:R2149-R2156.
- 584 Shobahah J, Xue SJ, Hu DB, Zhao C, Wei M, Quan YP, and Yu W. 2017. Quantitative
585 phosphoproteome on the silkworm (*Bombyx mori*) cells infected with baculovirus.
586 *Virology Journal* 14.
- 587 Tagua VG, Pausch M, Eckel M, Gutierrez G, Miralles-Duran A, Sanz C, Eslava AP, Pokorny R,
588 Corrochano LM, and Batschauer A. 2015. Fungal cryptochrome with DNA repair activity
589 reveals an early stage in cryptochrome evolution. *Proceedings Of the National Academy
590 Of Sciences Of the United States Of America* 112:15130-15135.
- 591 Takano Y, Kikuchi T, Kubo Y, Hamer JE, Mise K, and Furusawa I. 2000. The *Colletotrichum*
592 *lagenarium* MAP kinase gene CMK1 regulates diverse aspects of fungal pathogenesis.
593 *Molecular Plant-Microbe Interactions* 13:374-383.
- 594 Tang LH, Jian HH, Song CY, Bao DP, Shang XD, Wu DQ, Tan Q, and Zhang XH. 2013.
595 Transcriptome analysis of candidate genes and signaling pathways associated with light-
596 induced brown film formation in *Lentinula edodes*. *Appl Microbiol Biotechnol* 97:4977-
597 4989.
- 598 Tang LH, Tan Q, Bao DP, Zhang XH, Jian HH, Li Y, Yang RH, and Wang Y. 2016.
599 Comparative Proteomic Analysis of Light-Induced Mycelial Brown Film Formation in
600 *Lentinula edodes*. *Biomed Research International*.
- 601 Terashima K, Yuki K, Muraguchi H, Akiyama M, and Kamada T. 2005. The *dst1* gene involved
602 in mushroom photomorphogenesis of *Coprinus cinereus* encodes a putative photoreceptor
603 for blue light. *Genetics* 171:101-108.
- 604 Thingholm TE, Jensen ON, and Larsen MR. 2009. Analytical strategies for phosphoproteomics.
605 *Proteomics* 9:1451-1468.

- 606 Tsivileva OM, Pankratov AN, Nikitina VE, and Garibova LV. 2005. Effect of media components
607 on the mycelial film formation in submerged culture of *Lentinus edodes* (Shiitake). *Food*
608 *Technology And Biotechnology* 43:227-234.
- 609 van Wijk KJ, Friso G, Walther D, and Schulze WX. 2014. Meta-Analysis of *Arabidopsis*
610 *thaliana* Phospho-Proteomics Data Reveals Compartmentalization of Phosphorylation
611 Motifs. *Plant Cell* 26:2367-2389.
- 612 Varnai A, Makela MR, Djajadi DT, Rahikainen J, Hatakka A, and Viikari L. 2014.
613 Carbohydrate-Binding Modules of Fungal Cellulases: Occurrence in Nature, Function,
614 and Relevance in Industrial Biomass Conversion. *Advances In Applied Microbiology, Vol*
615 *88* 88:103-165.
- 616 Vidal-Melgosa S, Pedersen HL, Schuckel J, Arnal G, Dumon C, Amby DB, Monrad RN,
617 Westereng B, and Willats WGT. 2015. A New Versatile Microarray-based Method for
618 High Throughput Screening of Carbohydrate-active Enzymes. *Journal Of Biological*
619 *Chemistry* 290:9020-9036.
- 620 Wang K, Zhao Y, Li M, Gao F, Yang MK, Wang X, Li SQ, and Yang PF. 2014. Analysis of
621 phosphoproteome in rice pistil. *Proteomics* 14:2319-2334.
- 622 Wang X, Bian YY, Cheng K, Gu LF, Ye ML, Zou HF, Sun SSM, and He JX. 2013. A large-
623 scale protein phosphorylation analysis reveals novel phosphorylation motifs and
624 phosphoregulatory networks in *Arabidopsis*. *Journal of Proteomics* 78:486-498.
- 625 Weijn A, Bastiaan-Net S, Wichers HJ, and Mes JJ. 2013. Melanin biosynthesis pathway in
626 *Agaricus bisporus* mushrooms. *Fungal Genetics And Biology* 55:42-53.
- 627 Wilkens C, Busk PK, Pilgaard B, Zhang WJ, Nielsen KL, Nielsen PH, and Lange L. 2017.
628 Diversity of microbial carbohydrate-active enzymes in Danish anaerobic digesters fed
629 with wastewater treatment sludge. *Biotechnology for Biofuels* 10.
- 630 Wong MT, Wang WJ, Couturier M, Razeq FM, Lombard V, Lapebie P, Edwards EA, Terrapon
631 N, Henrissat B, and Master ER. 2017. Comparative Metagenomics of Cellulose- and
632 Poplar Hydrolysate-Degrading Microcosms from Gut Microflora of the Canadian Beaver
633 (*Castor canadensis*) and North American Moose (*Alces americanus*) after Long-Term
634 Enrichment. *Frontiers In Microbiology* 8.

- 635 Wu JY, Chen HB, Chen MJ, Kan SC, Shieh CJ, and Liu YC. 2013. Quantitative analysis of LED
636 effects on edible mushroom *Pleurotus eryngii* in solid and submerged cultures. *Journal*
637 *Of Chemical Technology And Biotechnology* 88:1841-1846.
- 638 Xie CL, Gong WB, Zhu ZH, Yan L, Hu ZX, and Peng YD. 2018. Comparative transcriptomics
639 of *Pleurotus eryngii* reveals blue-light regulation of carbohydrate-active enzymes
640 (CAZymes) expression at primordium differentiated into fruiting body stage. *Genomics*
641 110:201-209.
- 642 Yang C, Ma L, Ying Z, Jiang X, and Lin Y. Sequence Analysis and Expression of a Blue-light
643 Photoreceptor Gene, *Slwc-1* from the Cauliflower Mushroom *Sparassis latifolia*. *Current*
644 *Microbiology* 74:469-475.
- 645 Yang F, Xu B, Zhao SJ, Li JJ, Yang YJ, Tang XH, Wang F, Peng MZ, and Huang ZX. 2012. De
646 novo sequencing and analysis of the termite mushroom (*Termitomyces albuminosus*)
647 transcriptome to discover putative genes involved in bioactive component biosynthesis.
648 *Journal Of Bioscience And Bioengineering* 114:228-231.
- 649 Yin J, Xin XD, Weng YJ, and Gui ZZ. 2017. Transcriptome-wide analysis reveals the progress
650 of *Cordyceps militaris* subculture degeneration. *Plos One* 12.
- 651 Yoo SI, Lee HY, Markkandan K, Moon S, Ahn YJ, Ji S, Ko J, Kim SJ, Ryu H, and Hong CP. 2019. Comparative
652 transcriptome analysis identified candidate genes involved in mycelium browning in *Lentinula edodes*.
653 *BMC Genomics* 20:121. Yu CL, Wu QF, Sun CD, Tang ML, Sun JW, and Zhan YH. 2019.
654 The Phosphoproteomic Response of Okra (*Abelmoschus esculentus* L.) Seedlings to Salt
655 Stress. *International Journal Of Molecular Sciences* 20.
- 656 Yu JH, and Keller N. 2005. Regulation of secondary metabolism in filamentous fungi. *Annual*
657 *Review Of Phytopathology* 43:437-458.
- 658 Zerial M, and McBride H. 2001. Rab proteins as membrane organizers . *Nature Reviews*
659 *Molecular Cell Biology* 2:216-216.
- 660 Zhan Y, Wu Q, Chen Y, Tang M, Sun C, Sun J, and Yu C. 2019. Comparative proteomic
661 analysis of okra (*Abelmoschus esculentus* L.) seedlings under salt stress. 20:381.

- 662 Zhang CH, Dong WQ, Gen W, Xu BY, Shen CJ, and Yu CL. 2018. De Novo Transcriptome
663 Assembly and Characterization of the Synthesis Genes of Bioactive Constituents in
664 *Abelmoschus esculentus* (L.) Moench. *Genes* 9:16.
- 665 Zhang JJ, Chen H, Chen MJ, Ren A, Huang JC, Wang H, Zhao MW, and Feng ZY. 2015.
666 Cloning and functional analysis of a laccase gene during fruiting body formation in
667 *Hypsizygus marmoreus*. *Microbiological Research* 179:54-63.
- 668 Zhang M, Ma CY, Lv DW, Zhen SM, Li XH, and Yan YM. 2014. Comparative
669 Phosphoproteome Analysis of the Developing Grains in Bread Wheat (*Triticum aestivum*
670 L.) under Well-Watered and Water-Deficit Conditions. *Journal Of Proteome Research*
671 13:4281-4297.
- 672 Zhang XW, Li PR, Wang CL, Chen MH, Li ZJ, and Wang YR. 2013. Effect of Blue Light on the
673 Growth, Culture Morphology, and Pigment Production of *Monascus*. *Journal Of Pure*
674 *And Applied Microbiology* 7:671-678.
- 675 Zhou H, Ye M, Dong J, Corradini E, Cristobal A, Heck AJ, Zou H, and Mohammed S. 2013.
676 Robust phosphoproteome enrichment using monodisperse microsphere-based
677 immobilized titanium (IV) ion affinity chromatography. *Nat Protoc* 8:461-480.
- 678 Zhu XM, Liang S, Shi HB, Lu JP, Dong B, Liao QS, Lin FC, and Liu XH. 2018. VPS9 domain-
679 containing proteins are essential for autophagy and endocytosis in *Pyricularia oryzae*.
680 *Environ Microbiol* 20:1516-1530.
- 681
- 682

Figure 1

Figure 1 Overview of the phosphorylation proteomes.

(A) The pictures showed the fungal mycelia under different illumination for 22 days.

Experimental strategy for the quantitative analysis of phosphorylation proteomes from red and blue light treatment groups. (B) Pearson's correlation of the phosphorylation proteomes from two sample groups (three biological replicates for each group). (C) Basic statistical data of MS results. (D) Mass error distribution of all identified phosphorylated peptides. X-axis: Peptide Score; Y-axis: Peptides mass delta. (E) Length distribution of all identified phosphorylated peptides. X-axis: No. of Peptide; Y-axis: Peptide length.

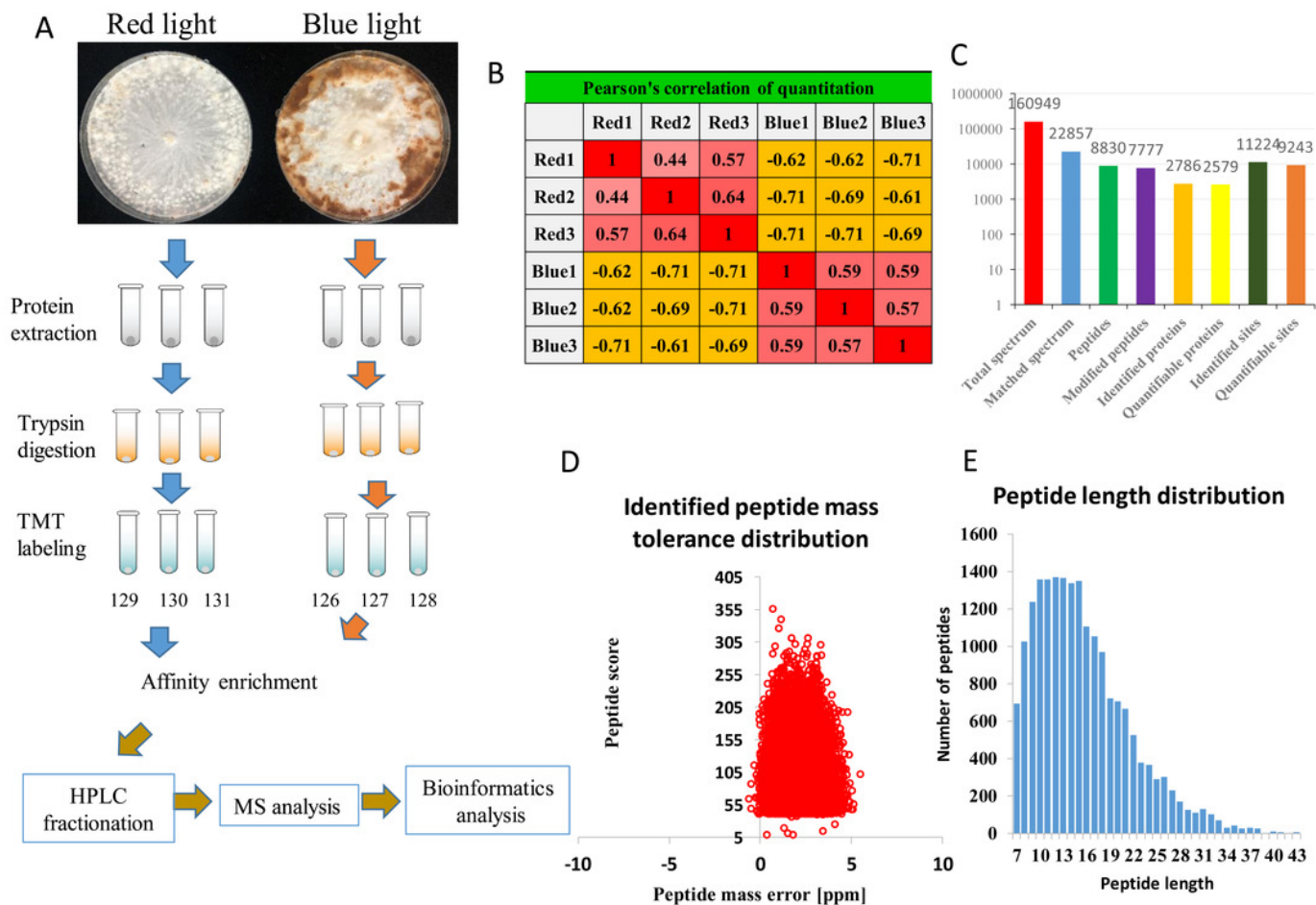


Figure 2

Figure 2 Analysis of the density of phosphorylation sites.

(A) Modification phosphorylated sites distribution of all identified peptides. (B) Comparison of the average densities of phosphorylation sites per protein among various species.

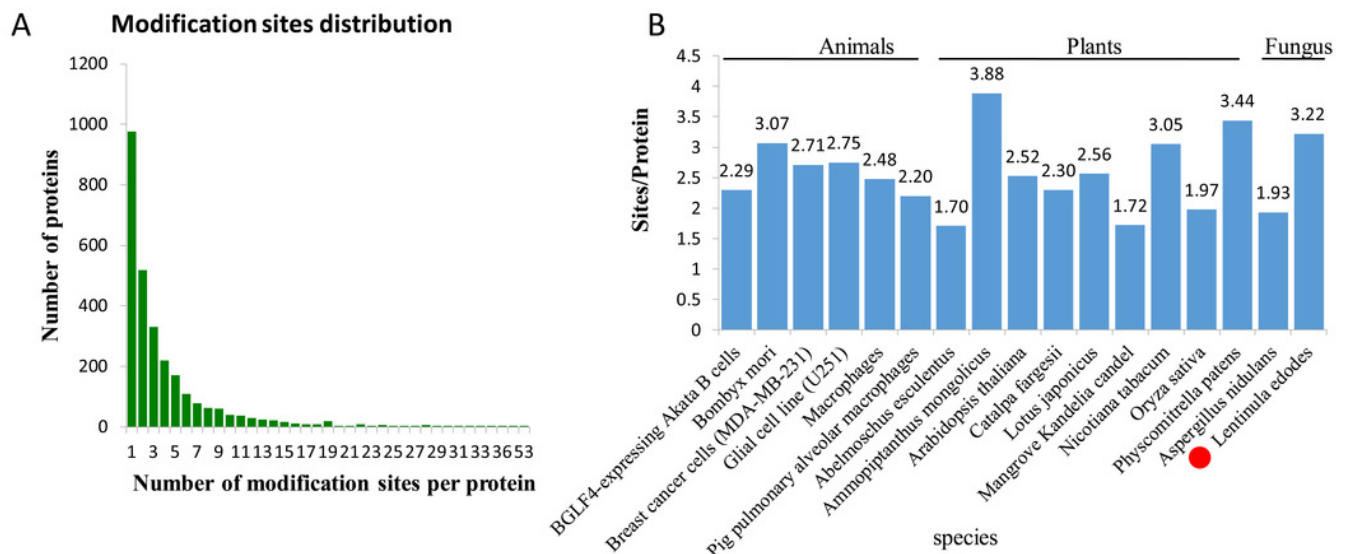


Figure 3

Figure 3 Annotation and classification of all identified phosphorylated proteins.

(A) GO analysis of all phosphorylated proteins. All proteins were classified by GO terms based on their biological process, cellular component and molecular function. (B) The euKaryotic Ortholog Groups annotation clustered all the phosphoproteins into four major categories: Information storage and processing, Cellular processes and signaling, Metabolism and Poorly characterized. (C) Subcellular locations of all identified phosphorylated proteins.

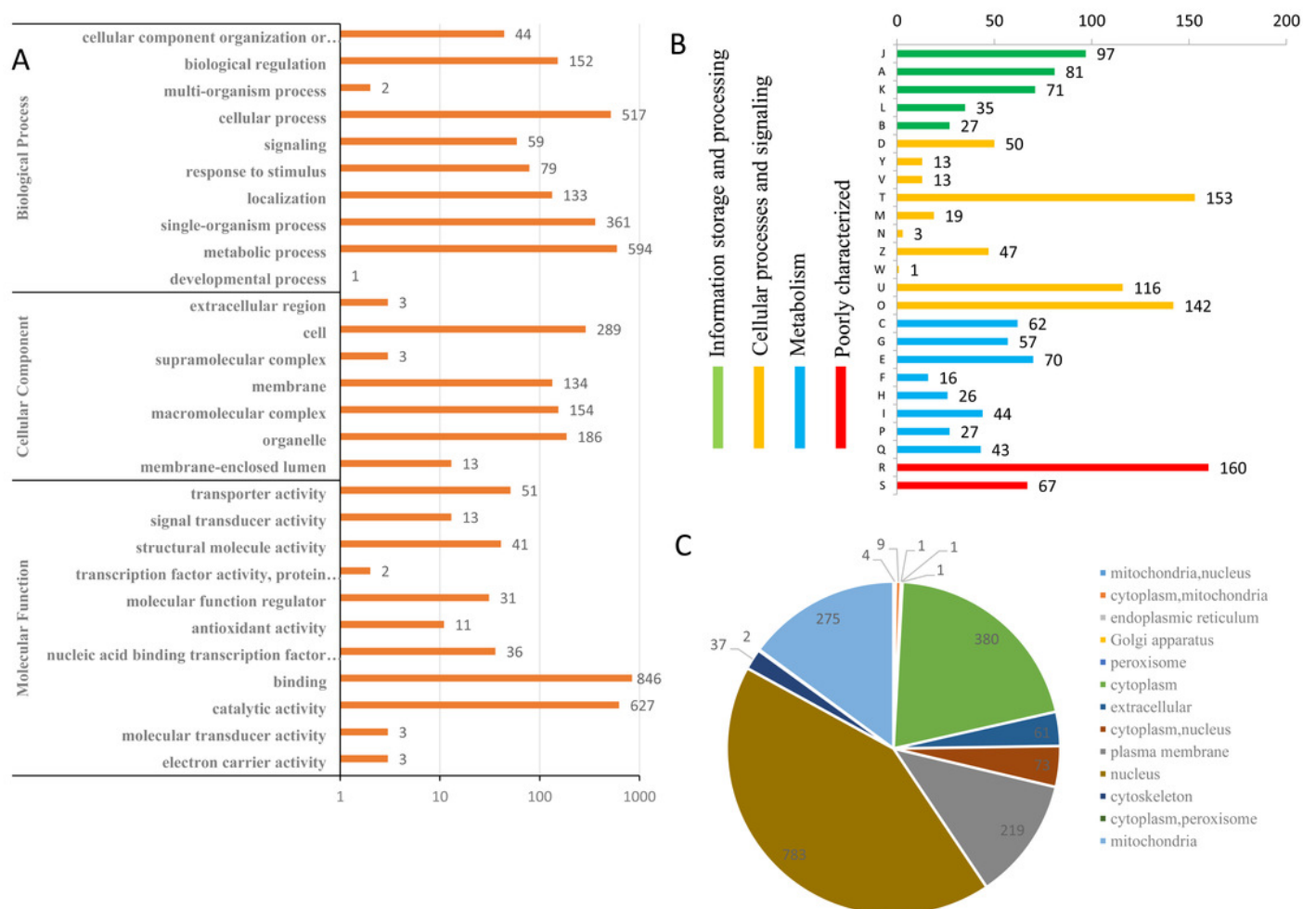


Figure 4

Figure 4 Phosphosite types and peptide motifs associated with phosphorylation.

(A) The distribution of phosphosites between serine, threonine and tyrosine residues. (B) Motif analysis of the amino acids surrounding the phosphosites. Sequence logo representation of 5 S-based and 5 T-based conserved phosphorylation motifs. (C) A plot showing the relative abundance of amino acids flanking a phosphorylated serine (S) and threonine (T) using the intensity map. Red indicated that this amino acid was significantly enriched near the modification site, and green indicated that this amino acid was significantly reduced near the modification site. Letters represent abbreviations for amino acids

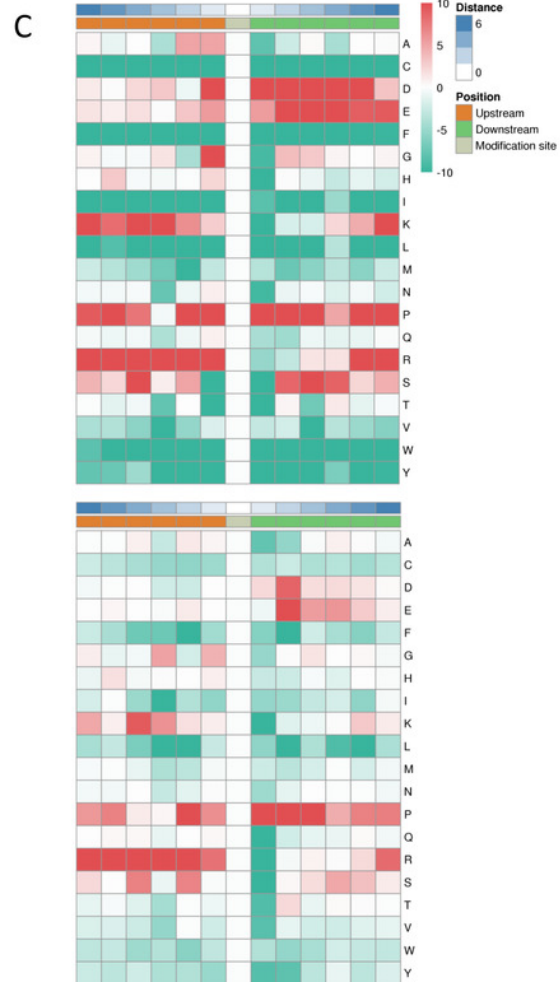
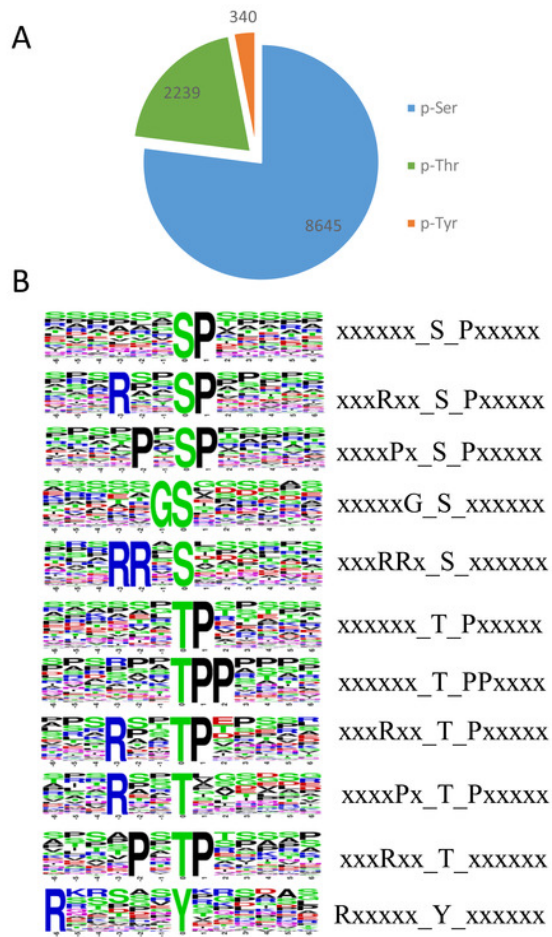


Figure 5

Figure 5 Impacts of illumination treatment on phosphorylation proteome levels in fungal mycelia.

(A) Heat map for the accumulation levels of all the identified phosphorylated proteins. Red indicates up-regulation and green indicates down-regulation. The heatmap scale ranges from 0 to +2. (B) The numbers of up- and down-regulated sites and proteins in red and blue light treatment comparison. (C) Subcellular locations of differentially phosphorylated proteins

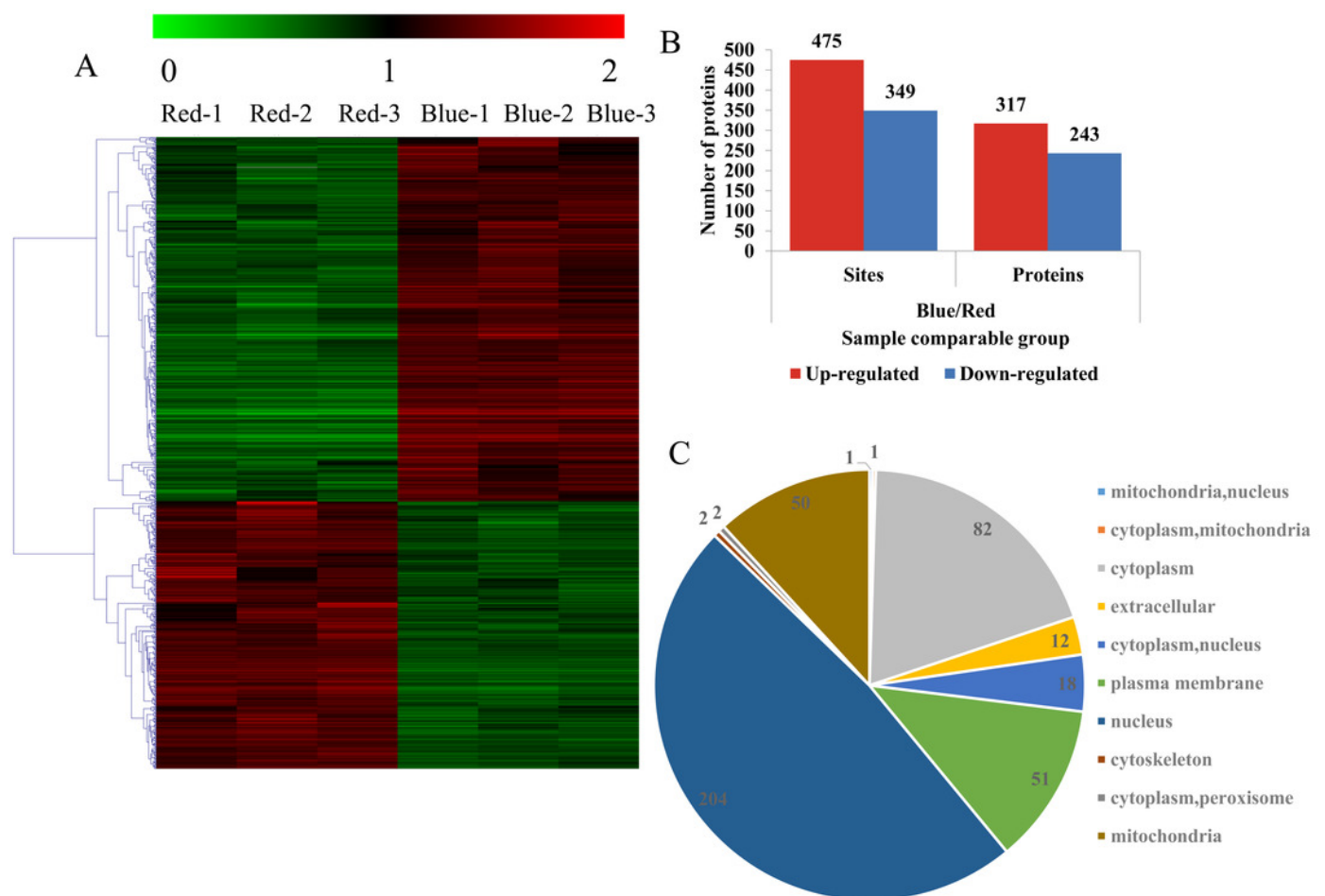


Figure 6

Figure 6 GO enrichment analysis of DPPs based on biological process (A), cellular component (B) and molecular function (C).

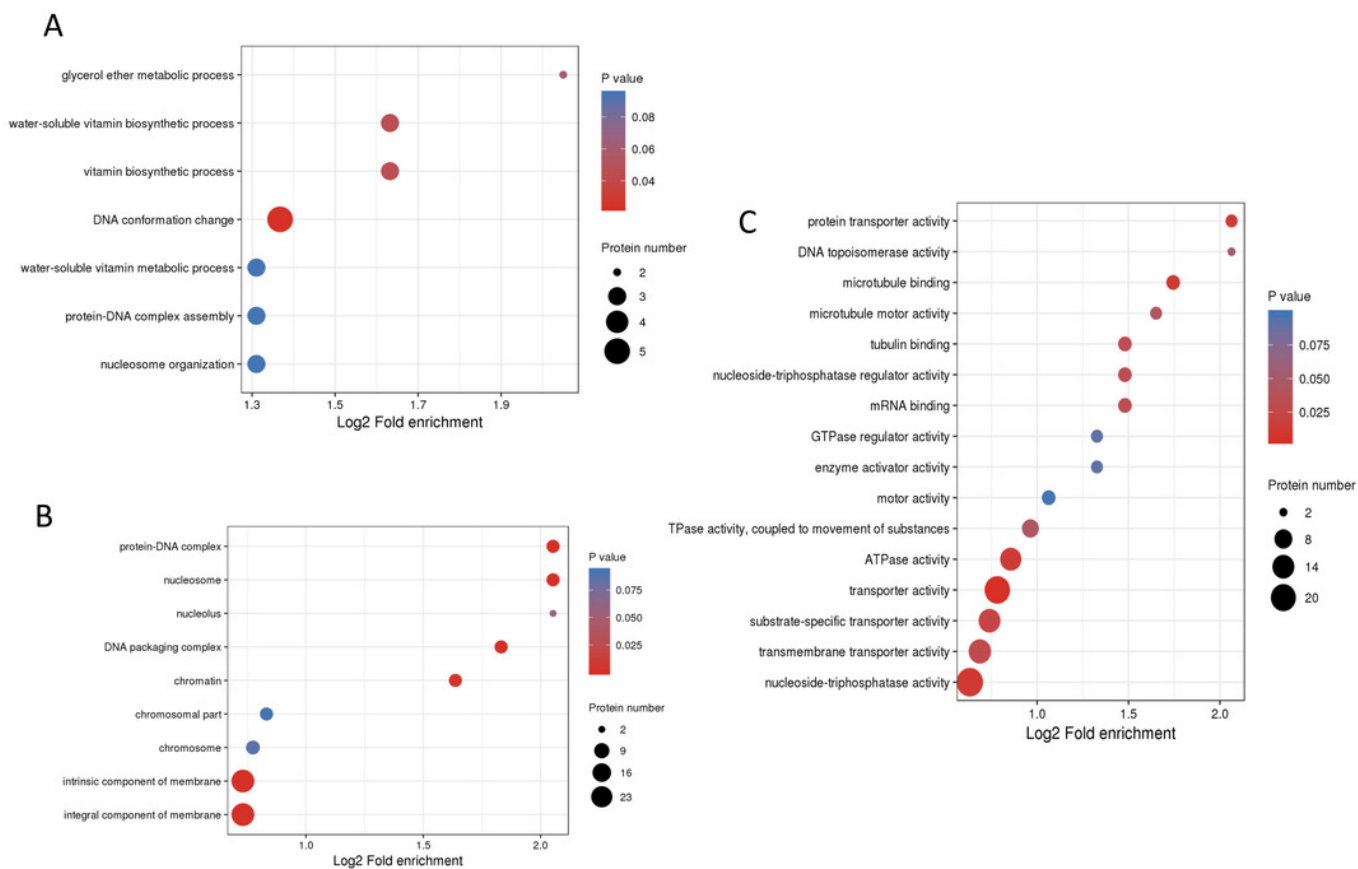


Table 1 (on next page)

Table 1. List of differentially expressed signal transduction mechanisms related phosphosites

1 **Table1.**List of differentially expressed signal transduction mechanisms related phosphosites

Protein accession	Position	Regulated Ratio	Type	P value	Amino acid	Protein description
A0A1Q3DXT2	147	2.041	Up	0.000701	S	Actin cytoskeleton-regulatory complex protein pan1
A0A1Q3DXT2	940	0.661	Down	0.0212	S	Actin cytoskeleton-regulatory complex protein pan1
A0A1Q3DXT2	340	1.566	Up	0.00104	S	Actin cytoskeleton-regulatory complex protein pan1
A0A1Q3DXT2	538	1.503	Up	0.000622	S	Actin cytoskeleton-regulatory complex protein pan1
A0A1Q3DXT2	145	2.041	Up	0.000701	S	Actin cytoskeleton-regulatory complex protein pan1
A0A1Q3DXT2	626	1.573	Up	0.00602	S	Actin cytoskeleton-regulatory complex protein pan1
A0A1Q3EQA0	342	0.666	Down	0.0269	S	Arf gtpase activator
A0A1Q3EH65	144	0.457	Down	0.00398	S	Carbohydrate-binding module family 21 protein
A0A1Q3EH65	184	0.46	Down	0.000337	S	Carbohydrate-binding module family 21 protein
A0A1Q3EH65	1114	0.634	Down	0.00106	S	Carbohydrate-binding module family 21 protein
A0A1Q3EH65	391	0.512	Down	0.0000778	S	Carbohydrate-binding module family 21 protein
A0A1Q3EIZ3	287	0.542	Down	0.0000823	S	Casein kinase II subunit beta
A0A1Q3EIZ3	363	0.472	Down	0.000779	S	Casein kinase II subunit beta
A0A1Q3EHC7	350	1.787	Up	0.0024	S	Ck1 ck1 ck1-d protein kinase
A0A1Q3EML6	60	0.596	Down	0.00757	S	Gtpase-activating protein gyp7

A0A1Q3DYV9	5	1.542 Up	0.00764 S	Guanine nucleotide-binding protein
A0A1Q3DYV9	220	1.778 Up	0.000163 S	Guanine nucleotide-binding protein
A0A1Q3EBC7	120	0.663 Down	0.00414 T	HCP-like protein
A0A1Q3EQ51	108	2.293 Up	0.0123 S	Kinase-like protein
A0A1Q3EEF5	191	0.653 Down	8.16E-07 Y	Map kinase
A0A1Q3EEF5	189	0.641 Down	1.16E-06 T	Map kinase
A0A1Q3EEF5	194	0.572 Down	0.0000373 T	Map kinase
A0A1Q3E4D7	4	0.566 Down	0.000739 Y	Mitogen activated protein kinase-like protein
A0A1Q3EII7	44	0.59 Down	0.00196 Y	mRNA stability protein OS=Lentinula edodes
A0A1Q3E829	28	0.651 Down	0.000319 Y	Neutral alkaline nonlysosomal ceramidase
A0A1Q3EKW8	21	1.828 Up	0.00182 S	Non-specific serine/threonine protein kinase
A0A1Q3EKW8	19	1.717 Up	0.0000797 S	Non-specific serine/threonine protein kinase
A0A1Q3E982	790	0.53 Down	0.023 S	Non-specific serine/threonine protein kinase
A0A1Q3E1S4	101	0.642 Down	0.00332 S	Otu-like cysteine
A0A1Q3E102	696	1.667 Up	0.0108 S	Phosphatidylinositol 3-kinase VPS34
A0A1Q3E326	400	0.496 Down	0.000677 S	Protein phosphatase 2c
A0A1Q3E326	588	0.554 Down	0.0000166 S	Protein phosphatase 2c
A0A1Q3E326	402	0.5 Down	0.0000243 T	Protein phosphatase 2c
A0A1Q3E326	586	0.51 Down	0.0000438 S	Protein phosphatase 2c
A0A1Q3E326	393	0.655 Down	0.00102 S	Protein phosphatase 2c
A0A1Q3EFR0	271	0.543 Down	0.000024 S	Protein serine threonine phosphatase 2C

A0A1Q3E8Y4	138	1.593 Up	0.000198 S	Ras guanyl-nucleotide exchange factor
A0A1Q3EIH9	765	0.636 Down	0.000277 S	Rho gtpase activator
A0A1Q3DW25	452	0.335 Down	0.000459 S	Serine threonine-protein kinase
A0A1Q3E8M7	137	0.648 Down	0.00158 S	SGS-domain-containing protein
A0A1Q3EKV3	265	1.703 Up	0.039 S	Signal transducer
A0A1Q3EKV3	267	2.602 Up	0.000018 Y	Signal transducer
A0A1Q3EKV3	263	2.391 Up	9.39E-07 S	Signal transducer OS=Lentinula edodes
A0A1Q3E1B1	1413	1.776 Up	0.0000573 S	Sin component scaffold protein cdc11
A0A1Q3DX25	818	0.602 Down	0.0273 S	TKL TKL-ccin protein kinase
A0A1Q3EHP8	698	2.269 Up	0.000503 S	Uncharacterized protein
A0A1Q3ECY7	1099	1.628 Up	0.000258 S	Uncharacterized protein
A0A1Q3EHP8	695	2.269 Up	0.000503 S	Uncharacterized protein
A0A1Q3E1M6	515	0.586 Down	0.00232 S	YTH domain-containing protein 1
A0A1Q3E1M6	531	0.639 Down	0.0227 S	YTH domain-containing protein 1

Table 2 (on next page)

Table 2. List of differentially expressed carbohydrateactive enzymes family phosphosites

Protein accession	Position	Ratio	Regulated Type	P value	Amino acid	Protein description
glycoside hydrolase						
A0A1Q3D VW4	888	1.522	Up	0.00618	S	Glycoside hydrolase family 105 protein
A0A1Q3D VY0	489	1.774	Up	0.000241	S	Glycoside hydrolase family 1 protein
A0A1Q3D VY0	481	1.508	Up	0.0398	S	Glycoside hydrolase family 1 protein
A0A1Q3E E19	429	1.931	Up	0.0000401	S	Glycoside hydrolase family 61 protein
carbohydrate-binding module						
A0A1Q3D XJ6	394	0.555	Down	0.0000212	T	Carbohydrate-binding module family 48
A0A1Q3D XJ6	396	0.556	Down	0.000962	T	Carbohydrate-binding module family 48
A0A1Q3D XJ6	377	0.483	Down	0.00000158	S	Carbohydrate-binding module family 48
A0A1Q3D XJ6	409	0.503	Down	0.0000161	S	Carbohydrate-binding module family 48
A0A1Q3D XJ6	380	0.508	Down	0.0000025	S	Carbohydrate-binding module family 48
A0A1Q3D XJ6	388	0.451	Down	0.0000568	S	Carbohydrate-binding module family 48
A0A1Q3E 7W8	134	0.561	Down	0.0000969	S	Carbohydrate-binding module family 12
A0A1Q3E H65	1114	0.634	Down	0.00106	S	Carbohydrate-binding module family 21
A0A1Q3E H65	391	0.512	Down	0.0000778	S	Carbohydrate-binding module family 21
A0A1Q3E H65	184	0.46	Down	0.000337	S	Carbohydrate-binding module family 21
A0A1Q3E H65	144	0.457	Down	0.00398	S	Carbohydrate-binding module family 21
carbohydrate esterase						
A0A1Q3E 195	171	0.312	Down	0.000639	S	Lipase from carbohydrate esterase family ce10
A0A1Q3E GY1	39	0.605	Down	0.000116	T	Lipase from carbohydrate esterase family ce10

glycosyl transferase

A0A1Q3DXW9	1240	1.663	Up	0.000342	S	Glycosyltransferase family 20 protein
A0A1Q3E591	146	0.655	Down	0.00272	T	Glycosyltransferase family 4 protein
A0A1Q3E591	24	2.532	Up	0.0291	S	Glycosyltransferase family 4 protein
A0A1Q3EH60	1581	1.585	Up	0.000836	S	Glycosyltransferase family 2 protein
A0A1Q3EI36	235	0.64	Down	0.009	S	Glycosyltransferase Family 22 protein
A0A1Q3ERC2	75	0.622	Down	0.00812	T	Glycosyltransferase family 2 protein

1 **Table2.** List of differentially expressed carbohydrateactive enzymes family phosphosites